Lattice Monte Carlo simulations of FePt nanoparticles: Influence of size, composition, and surface segregation on order-disorder phenomena

Michael Müller* and Karsten Albe
Institut für Materialwissenschaft, Technische Universität Darmstadt, D-64287 Darmstadt, Germany
(Received 23 March 2005; revised manuscript received 22 July 2005; published 9 September 2005)

Order-disorder phenomena in FePt nanoparticles are investigated by lattice Monte Carlo computer simulations. The Metropolis algorithm is applied based on particle exchange and configurational energies that are calculated by an Ising Hamiltonian including nearest- and next-nearest-neighbor interactions. The adjustable parameters were determined from the bulk phase diagram and experiments on surface segregation of FePt thin films. By monitoring the long-range order parameter we study the influence of size, composition and surface segregation on the order-disorder transition. Our results reveal a distinct segregation behavior for nonstoichiometric compositions. Platinum atoms in excess exhibit a clear tendency for complete surface segregation on edge positions and (100) facets. Excess iron atoms, in contrast, tend to preferentially alloy in the bulk and on (100) facets. For a given particle size and variations in composition of ±4% in maximum, the transition temperature is lowered by less than 50 K, but more pronounced for excess Fe than Pt. For a fixed composition and varying size, in contrast, the transition temperature is lowered by 40 to 380 K compared to the bulk value for particle diameters ranging from 8.5 to 2.5 nm. Nevertheless, for temperatures below 1100 K, the ordered phase is the thermodynamically stable phase for all particle sizes. The most pronounced effect on the ordering behavior is observed, if surface segregation tendencies are systematically modified. If one element is fully occupying the outer surface layer, we observe the formation of internal disorder and the formation of $L1_2$ domains. By increasing the concentration of the segregating element and thus readjusting the stoichiometric composition in the bulk, the order in the particles can be restored.

DOI: 10.1103/PhysRevB.72.094203 PACS number(s): 61.46.+w, 64.60.Cn, 64.70.Nd

I. INTRODUCTION

FePt nanoparticles in the hard magnetic $L1_0$ phase are a candidate material for the next generation of high-density recording media. In the past, a large number of experimental methods for the synthesis of free and supported FePt nanoparticles were explored including attempts to prepare two-dimensional particle arrays (see, e.g., Refs. 1–3).

While the ordered structure with its large magnetocrystalline anisotropy is the thermodynamically stable phase at low temperatures, the bulk phase diagram of FePt reveals an order-disorder transition to a disordered fcc phase at about 1573 K. Interestingly, there is a number of experimental studies that observe this disordered phase in FePt nanoparticles even after temperature treatment[4,5] and it is still a matter of debate, whether this is a result of kinetic processes or equilibrium thermodynamics.

In fact, it is well known that in the nanometer range particle size has to be considered as an additional thermodynamic variable, which directly affects equilibrium properties. This is because particle shape, crystallographic structure, and local composition can significantly vary with size. Moreover, particles supported by a substrate or covered by ligands can again reveal different behavior. In order to optimize experimental processes, it is therefore highly desirable to gain a detailed understanding of the thermodynamics of FePt particles on the nanometer scale.

In this work, we have therefore studied order-disorder phenomena in FePt nanoparticles as a function of size and composition. Because of the structural similarities of the $L1_0$ and fcc phase we can apply a lattice Monte Carlo model. The key ingredient is an Ising-type Hamiltonian that includes not only nearest-neighbor interactions, but also next-nearest neighbors. This feature is essential to correctly describe the bulk phase diagram and energy of antiphase boundaries (see Sec. II). By applying the particle exchange mechanism within a Metropolis Monte Carlo scheme we can explore the equilibrium structure of particles with varying size and composition at given temperatures.

II. MODEL

In our simulations, bulk FePt alloys and FePt alloy nanoparticles are described by applying an Ising-type Hamiltonian on a rigid fcc lattice: Each site of the lattice can be occupied by either an Fe or Pt atom. Atom-atom interactions are restricted to nearest-neighbor (NN) and next-nearest-neighbor (NNN) pairs and are described by pair interaction energies $\varepsilon_1^{\mathrm{FeFe}}$, $\varepsilon_1^{\mathrm{PtPt}}$, $\varepsilon_1^{\mathrm{FePt}}$ (for NN pairs) and $\varepsilon_2^{\mathrm{FeFe}}$, $\varepsilon_2^{\mathrm{PtPt}}$, $\varepsilon_2^{\mathrm{FePt}}$ (for NNN pairs). The configurational energy of a system is then given by

$$E = \sum_i \left(\sum_{\mathrm{NN}j} \frac{1}{2} \varepsilon_1^{ij} + \sum_{\mathrm{NNN}j} \frac{1}{2} \varepsilon_2^{ij} \right), \tag{1}$$

where the first sum runs over all atoms i, the second and third sum over all NN and NNN atoms of atom i. The ordering properties of this model do not depend on the absolute values of the individual pair interaction energies, but only on a number of linear combinations of them. At the end, the number of adjustable parameters is reduced to the following quantities:

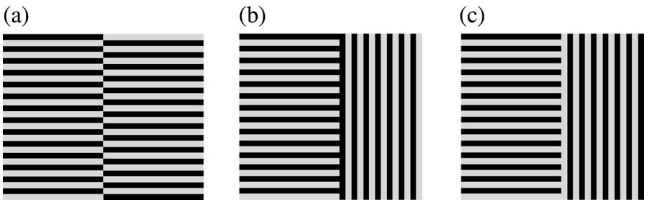

FIG. 1. Illustration of antiphase boundaries of the $L1_0$ ordered phase: (a) conservative antiphase boundary, (b) and (c) nonconservative antiphase boundary. Black stripes denote Fe layers, gray stripes denote Pt layers.

$$J_1 = \frac{1}{4}\varepsilon_1^{\mathrm{FeFe}} + \frac{1}{4}\varepsilon_1^{\mathrm{PtPt}} - \frac{1}{2}\varepsilon_1^{\mathrm{FePt}}, \tag{2}$$

$$J_2 = \frac{1}{4}\varepsilon_2^{\mathrm{FeFe}} + \frac{1}{4}\varepsilon_2^{\mathrm{PtPt}} - \frac{1}{2}\varepsilon_2^{\mathrm{FePt}}, \tag{3}$$

$$h = 3\varepsilon_1^{\mathrm{FeFe}} - 3\varepsilon_1^{\mathrm{PtPt}} + \frac{3}{2}\varepsilon_2^{\mathrm{FeFe}} - \frac{3}{2}\varepsilon_2^{\mathrm{PtPt}}. \tag{4}$$

For a bulk system with fixed composition, only the parameters J_1 and J_2 determine the ordering behavior, as they define the energy change for exchanging Fe and Pt atoms. For a system with free surfaces, the difference between the interaction energies of like atoms ($\varepsilon_1^{\mathrm{FeFe}} - \varepsilon_1^{\mathrm{PtPt}}$ and $\varepsilon_2^{\mathrm{FeFe}} - \varepsilon_2^{\mathrm{PtPt}}$) also plays an important role. Depending on whether Fe-Fe or Pt—Pt bonds are stronger, Pt or Fe atoms tend to segregate on the surface. Therefore, the parameter h determines the segregation behavior of the system.

The complete analogy of this model to an Ising model is established by describing the occupation of the lattice by a variable s_k. The variable is defined to have the value 1 if site k is occupied by an Fe atom and -1 if site k is occupied by a Pt atom. Then the Hamiltonian can be expressed for a bulk system by

$$H = J_1 \sum_{\mathrm{NN}\langle k,l\rangle} s_k s_l + J_2 \sum_{\mathrm{NNN}\langle k,l\rangle} s_k s_l + h \sum_k s_k. \tag{5}$$

Here, the first and second sums run over all pairs of NN and NNN sites, respectively. The third sum runs over all lattice sites. For a system with free surfaces, the Hamiltonian in the spinlike notation becomes more complex, since summations over all sites in surface layers have to be included. Therefore, Eq. (1) is preferred in this work.

As depicted in Fig. 1, two types of antiphase boundaries (APBs) can occur on an $L1_0$ ordered lattice, namely, conservative and nonconservative APBs. The energy contents of the APBs resulting from our model are listed in Table I. For $J_2 = 0$, the conservative APB has no energy penalty, since the number of NN bonds between like and unlike atoms does not change by introducing a conservative APB into an ordered structure. In result, the ground state of the Ising model without NNN interactions is highly degenerate. Therefore, the inclusion of NNN interactions is an indispensable feature for modelling order-disorder transitions in single domain particles of FePt that possess little or no APBs. In order to keep the model as simple as possible, we restrict the NNN interactions to unlike atoms only by setting parameters $\varepsilon_2^{\mathrm{FeFe}}$ and $\varepsilon_2^{\mathrm{PtPt}}$ to zero.

TABLE I. APB energies (γ) expressed by the model parameters. a_0 is the lattice parameter of the fcc unit cell.

APB	$\gamma \cdot a_0^2$
conservative [Fig. 1(a)]	$-8J_2$
nonconservative [Fig. 1(b)]	$4J_1 - 4J_2 + \frac{2}{3}h$
nonconservative [Fig. 1(c)]	$4J_1 - 4J_2 - \frac{2}{3}h$

For a quantitative description of the order in the system, we use a three component long-range order (LRO) parameter $\underline{\Psi}$,[6] which is defined as follows: The fcc lattice can be decomposed into four simple cubic sublattices ν. A sublattice occupation m_ν is then defined as

$$m_\nu = 1/N \sum_{k\in\nu} s_k, \quad \nu = 1,2,3,4. \tag{6}$$

The summation in Eq. (6) is over all sites of the sublattice ν. N is the number of atoms in the system. The components of the order parameter are then defined as

$$\underline{\psi} = \begin{pmatrix} \psi_1 \\ \psi_2 \\ \psi_3 \end{pmatrix} = \begin{pmatrix} m_1 + m_2 - m_3 - m_4 \\ m_1 - m_2 - m_3 + m_4 \\ m_1 + m_2 + m_3 - m_4 \end{pmatrix}. \tag{7}$$

The LRO parameter takes the values $(\pm 1\ 0\ 0)$, $(0\ \pm 1\ 0)$, $(0\ 0\ \pm 1)$ for complete $L1_0$ ordering in x, y, and z directions, respectively. Complete $L1_2$ ordering is indicated by the values $(\pm\frac{1}{2}\ \pm\frac{1}{2}\ \pm\frac{1}{2})$, $(\pm\frac{1}{2}\ \mp\frac{1}{2}\ \pm\frac{1}{2})$, $(\mp\frac{1}{2}\ \pm\frac{1}{2}\ \mp\frac{1}{2})$, and $(\mp\frac{1}{2}\ \mp\frac{1}{2}\ \pm\frac{1}{2})$.

By taking the ordering direction (c axis of the $L1_0$ phase) parallel to the z axis of the coordinate system, it is finally sufficient to only monitor the z component of $\underline{\psi}$ for analyzing order-disorder transitions. The LRO parameter discussed in the remainder of this paper is therefore identical to ψ_3.

III. MC SIMULATIONS

A. Simulation method

In order to determine equilibrium properties of our model system, we apply a standard particle exchange Monte Carlo scheme. At each elementary step of the MC simulations, a pair of two neighboring atoms is picked randomly and the energy change for an exchange of the two atoms is calculated. The exchange is then accepted or declined according to the Metropolis algorithm. After the system has reached equilibrium from an arbitrarily chosen initial configuration, properties of interest (e.g., ordering, segregation) are sampled over a large number of MC steps. One MC step corresponds to N attempted exchanges of neighboring atoms, where N is the total number of atoms.

B. Fitting of the model parameters

1. FePt phase diagram

We determined the model parameters J_1 and J_2 by adjusting the phase diagram of our model system to the bulk phase

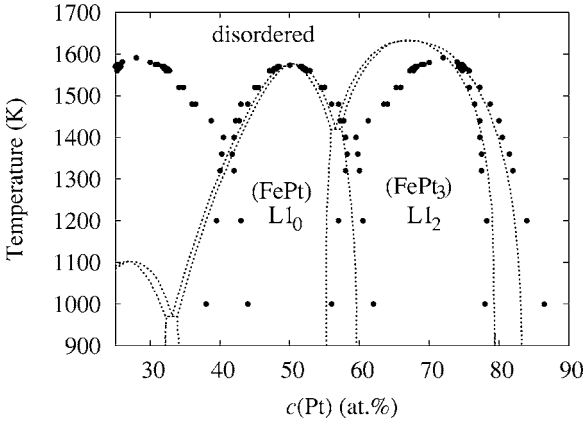

FIG. 2. Comparison of the phase diagram of our model (full circles) with the experimentally determined FePt phase diagram (dashed lines). The experimental phase diagram is plotted using data from Ref. 10.

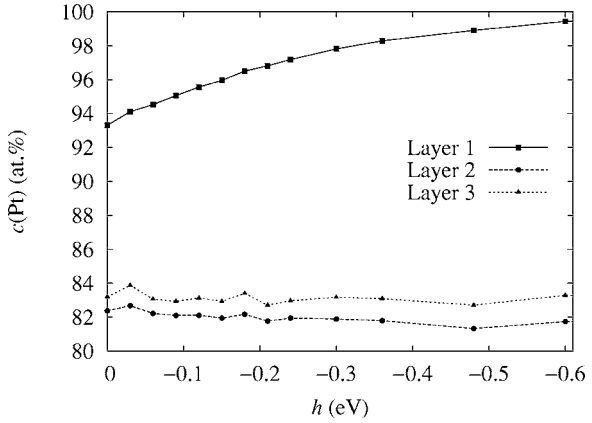

FIG. 3. Influence of the model parameter h on the segregation of Pt at the (111) surface of an $Fe_{20}Pt_{80}$ alloy at 1200 K.

diagram of FePt. In doing so, we used a bulk fcc lattice with 13 500 sites ($15\times15\times15$ unit cells) and periodic boundary conditions in x, y, and z directions. For fixed ratios $\alpha=J_2/J_1=0,0.05,0.1,0.15,0.2$ we varied J_1 until the correct ordering temperature of 1573 K was reproduced at the stoichiometric composition of $Fe_{50}Pt_{50}$: Starting with a completely disordered lattice, we run the simulation for 300 000 MC steps at 1585 K and then lowered the temperature by steps of 5 to 1500 K. The final structure of each simulation was used as input structure for the simulation at the next lower temperature.[7] The transition from the disordered to the ordered state was detected by monitoring the LRO parameter and J_1 was varied until the transition was situated in the temperature interval between 1575 and 1570 K. We verified that the results are independent of the input structures by repeating the temperature series for the best fit with completely ordered as well as disordered input structures at each temperature. We then determined the boundaries of the $L1_0$ ordered ($Fe_{50}Pt_{50}$) and $L1_2$ ordered ($Fe_{25}Pt_{75}$) phases for the given values of α and J_1: Close to the stoichiometric compositions, the ordering temperature was determined by running simulations with fixed composition at different temperatures following the same procedure as described before. The phase boundaries at compositions farther away from stoichiometry were determined by MC simulations in the grand-canonical ensemble, a method described in detail in Ref. 6. The best fit was obtained for $\alpha=0.2$, $J_1=0.0465$ eV, which gives $J_2=-0.0093$ eV. A comparison of the experimentally determined phase diagram and the phase diagram of our model is shown in Fig. 2.

An intrinsic feature of the Ising model with pair interaction energies is the symmetry of the phase diagram relative to the $Fe_{50}Pt_{50}$ composition.[8] Therefore, the model cannot reproduce all details of the asymmetric FePt phase diagram for all three ordered phases. Reproducing the asymmetry would require the inclusion of many-body interactions.[9] However, in the composition range of the particles considered in this work (46–54 at. % Pt), the stability region of the $L1_0$ ordered phase is matched very well by the pair-interaction model. The model also reproduces the two phase region separating the $L1_2$ ordered $FePt_3$ phase from the disordered substitutional Pt-rich solid solution. This feature is important, since the surface segregation behavior of the model is fitted at the composition $Fe_{20}Pt_{80}$, as described in the next section.

2. Surface segregation

With J_1 and J_2 fixed, the parameter h was determined by fitting our model to experimental results on surface segregation in thin films. Quantitative studies of the segregation behavior of FePt systems exist for the (111) surface of an $Fe_{20}Pt_{80}$ alloy.[11,12] It was found that at 1200 K, the (111) surface is enriched with Pt: the first layer consists of almost pure Pt [concentration 96±4 at. % (Ref. 11)]. The Pt concentration in the second and third layer is also increased [84±7 and 85±15 at. %,[11] respectively]. The dependence of Pt segregation on the parameter h has been analyzed by using an fcc lattice with free (111) surfaces in the z direction and periodic boundaries in x and y directions. The lattice consisted of 150 (111) layers with 1920 atoms per layer. The large number of (111) layers was necessary in order to make the two surfaces independent from each other. For each value of the parameter h, the lattice was initialized with a random distribution of Fe and Pt atoms in the ratio 20/80. The concentration profile was then determined by taking the average over 90 000 MC steps, after discarding the first 10 000 MC steps. In all simulations, the temperature was set to 1200 K. Figure 3 shows the Pt concentration in the first three surface layers as a function of the parameter h. As an effect of the ordering of the system,[12] Pt is enriched in the first surface layer to approximately 93 at. %, even without a driving force for surface segregation ($h=0$). With increasing h, the Pt concentration in the first layer increases to almost 100 at. %. In contrast to the first layer, the Pt concentrations in the second and third layer hardly depend on the parameter h. However, Pt is enriched to approximately 82 at. % in the second and 83 at. % in the third layer. The experimental result of 96 at. % Pt in the first surface layer is reproduced best with the parameter $h=-0.15$ eV. The concentration profile corresponding to this best fit is compared to the experimentally determined profile in Fig. 4. The model exactly reproduces

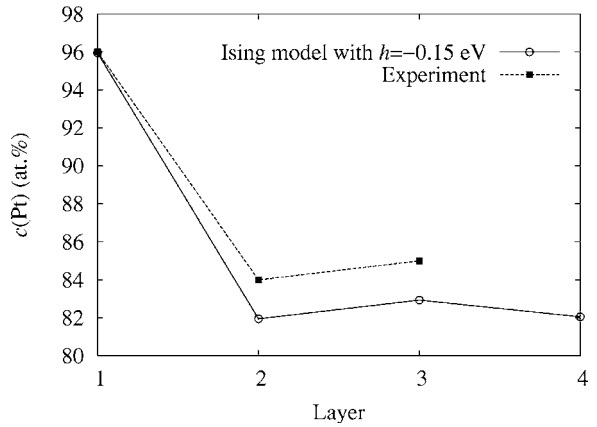

FIG. 4. Depth profile of the Pt concentration at the (111) surface of an $Fe_{20}Pt_{80}$ alloy at 1200 K. Comparison of experiments with the results of our model for $h=-0.15$ eV.

the Pt segregation in the first surface layer. It is also very reasonable for the second and third layers, where the calculated concentrations deviate from the experimental values by less than 2 at. %. The final set of model parameters is shown in Table II.

C. Particle shape

1. Experimental findings

Nanometer sized particles can exhibit a variety of size dependent conformations.[13,14] In the case of single crystalline fcc metal particles, the thermodynamically stable shape is determined by a Wulff construction. It resembles a truncated octahedron or cuboctahedron, depending on the ratio of the (111) and (100) facet sizes.[14] In addition single crystalline particles, pure fcc metal clusters often exhibit multiply twinned structures, which manifest themselves in icosahedral or decahedral particles solely terminated by pseudo-(111) surfaces.[13] Atomistic simulations[15,16] suggest that multiply twinned structures are energetically favored for small metallic clusters, since the reduced surface energy overcompensates the elastic energy introduced by twinning of the particle core. In contrast, single crystalline particles become the most stable phase for larger sizes, as the surface to volume ratio diminishes. Recently, this size-dependent structural transition was experimentally observed for pure Cu (Ref. 17) as well as Au (Ref. 18) nanoparticles.

TABLE II. Parameters for the Ising-type Hamiltonian.

Parameter	Value (eV)	Parameter	Value (eV)
J_1	0.0465	$\varepsilon_1^{\mathrm{FeFe}}$	0
J_2	−0.0093	$\varepsilon_1^{\mathrm{PtPt}}$	0.05
h	−0.15	$\varepsilon_1^{\mathrm{FePt}}$	−0.068
		$\varepsilon_2^{\mathrm{FeFe}}$	0
		$\varepsilon_2^{\mathrm{PtPt}}$	0
		$\varepsilon_2^{\mathrm{FePt}}$	0.0186

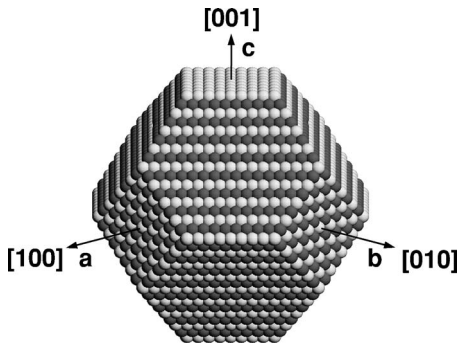

FIG. 5. Illustration of a completely $L1_0$ ordered regular truncated octahedron with 9201 atoms ($d=6.3$ nm).

In case of nanoalloys, experiments indicate that a similar behavior can also be found for FePt:FePt nanoparticles with a diameter of 5.9 nm prepared by gas-phase condensation show multiply twinned structures, while larger particles with a diameter of 7.6 nm prepared at higher gas pressures are single crystalline.[3] The shape of single crystalline particles with $L1_0$ structure was identified to be truncated octahedral or cuboctahedral.[19,20] In contrast to particles prepared from the gas phase, wet chemically processed FePt particles with surfaces modified by organic ligands are observed to be single crystalline down to sizes smaller than 3 nm in diameter.[4]

2. Monte Carlo model

The lattice Monte Carlo approach restricts our model to regular lattice positions and does not allow one to include structural transitions from single crystalline to multiply twinned particles. We therefore only consider single crystalline particles with regular truncated octahedral shape, which is characteristic for wet chemically processed FePt particles and particles prepared by gas phase condensation with a diameter larger than approximately 6 nm. For smaller particle sizes, where twinning can occur, the results of our simulations may not correctly describe particles prepared from the gas phase.

As a further simplification, the shape of the particles [i.e., the ratio of (111) to (100) facet sizes] does not change during the simulations, since no exchanges between atoms and unoccupied sites (vacancies) are allowed. In principle, the model can be expanded to also include changes of particle shape by allowing atom-vacancy exchanges and by adjusting the interaction energies $\varepsilon_1^{\mathrm{FeFe}}$ and $\varepsilon_1^{\mathrm{PtPt}}$ according to the surface energies of Fe and Pt. However, in contrast to atom-atom exchanges, atom-vacancy exchanges lead to a change in coordination number, and are thus accompanied by a much higher energy barrier. Consequently, atom-vacancy exchanges have a small probability in the MC algorithm and equilibrating internal order and particle shape simultaneously requires a much larger number of MC steps.

Figure 5 shows an ideally $L1_0$ ordered regular truncated octahedron (TO) with 9201 atoms (diameter $d=6.3$ nm). The surface of the TO consists of 8 (111) and 6 (100) facets. If the $L1_0$ structure is ordered along the crystallographic c direction, then the two (001) facets are occupied by either pure

TABLE III. Correlation between particle size and number of atoms for regular truncated octahedral shaped particles.

Diameter (nm)	Number of atoms
2.5	586
3.3	1289
4.0	2406
4.8	4033
5.5	6266
6.3	9201
7.0	12934
7.8	17561
8.5	23178

Fe or pure Pt, depending on whether the ordered structure starts with an Fe or Pt layer. The (100) and (010) facets are occupied by the same amount of Fe and Pt atoms (not counting the edges). An edge at the junction of two facets can also be occupied by either pure Fe or pure Pt, or can be alternately occupied by Fe and Pt atoms.

The composition of an ideally $L1_0$ ordered regular TO deviates from perfect stoichiometry because of constrictions imposed by the lattice structure and particle shape. Depending on whether the (001) facets are pure Fe or Pt, the overall concentration of Fe (Pt) is 51.54 at. % for a TO with 586 atoms (d=2.5 nm). With increasing size, this deviation decreases and the concentration of Fe (Pt) reaches 50.31 at. % for a TO with 23 178 atoms (d=8.5 nm).

D. Particle simulations

In order to analyze the dependence of ordering on particle size and composition, we considered particles of truncated octahedral shape containing 586 to 23 178 atoms, which corresponds to diameters of 2.5 to 8.5 nm. The correlation between particle size and number of atoms is listed in Table III. The composition of the particles was varied in the range from approximately 46 to 54 at. % Pt.

For each particle size and composition, we run a series of MC simulations at temperatures ranging from 300 to 1575 K. We start the series at the highest temperature, using a completely disordered particle as input structure. The output of the simulation is then handed over as input structure for the next lower temperature. At each temperature, configurations are sampled at least over 90 000 MC steps, after discarding the first 10 000 MC steps.

IV. RESULTS AND DISCUSSION

A. Ordering and surface segregation behavior

To begin with, we studied the dependence of particle structure on composition at 300 K. At this point, we will only report results for the 7.0 nm (12934 atoms) particle, since this is representative for all other particle sizes, too. Typical configurations for varying compositions at 300 K are shown in Fig. 6. At all compositions, the particles are $L1_0$ ordered single domain particles free of antiphase boundaries. The expected absence of APBs in the particles is because of NNN interactions ($J_2<0$) in the Ising model, which render conservative APBs energetically unfavorable: Simulations without NNN interactions ($J_2=0$), in contrast, produced ordered particles with an unrealistically large number of conservative APBs.

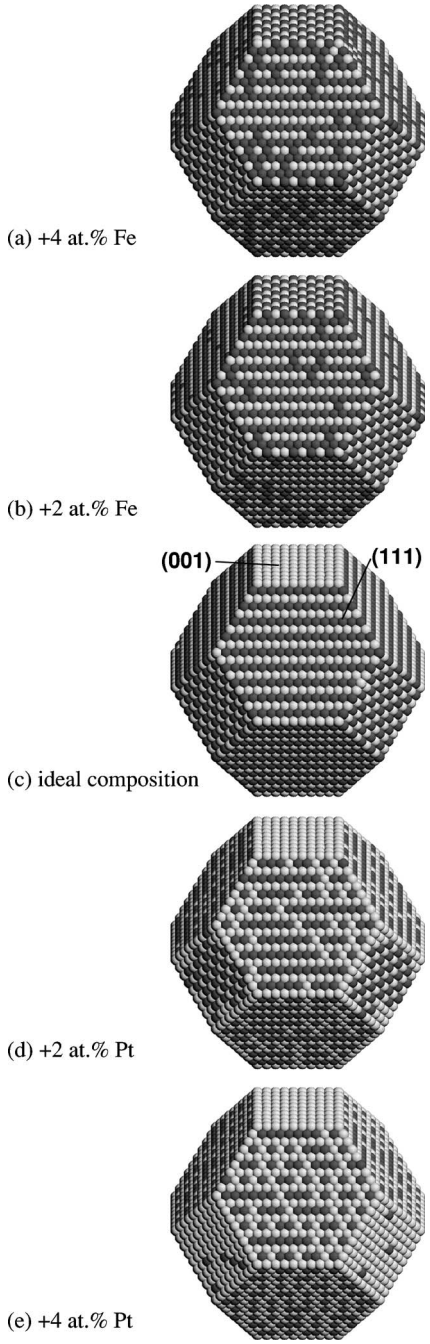

FIG. 6. Structure of particles with d=7.0 nm (12 934 atoms) after simulation at 300 K. The particle concentration varies from +4 at. % Fe to +4 at. % Pt relative to the concentration of an ideally ordered TO. Pt atoms are displayed light gray, Fe atoms dark gray.

If the c axis of the $L1_0$ phase is taken parallel to the [001] direction, then (001) planes are occupied alternatingly by Fe and Pt atoms. Because of the tendency of Pt atoms to segre-

TABLE IV. Energies for replacing an Fe atom by an excess Pt atom at different sites of an ideally $L1_0$ ordered regular TO.

Site	ΔE	ΔE (eV)
Volume	$8J_1-2h-12J_2$	0.7836
(111) Surface	$6J_1-\frac{3}{2}h-6J_2$	0.5598
(100) Surface	$8J_1-\frac{4}{3}h-10J_2$	0.665
(111)/(111) Edge	$6J_1-\frac{7}{6}h-4J_2$	0.4912
(100)/(111) Edge	$6J_1-\frac{7}{6}h-4J_2$	0.4912
Corner	$4J_1-h-4J_2$	0.3732

gate on the surface ($h<0$), the outer (001) facets of the particle are either fully occupied by Pt atoms [Figs. 6(c) and 6(d)] or are enriched with Pt, even if Fe atoms are available in excess [Figs. 6(a) and 6(b)]. Therefore, independent of composition, the ordered structure of all particles exhibits a Pt-Fe-$\cdots$-Fe-Pt stacking sequence in the [001] direction.

This observation is a direct consequence of the tendency of Pt atoms to segregate on the surface ($h<0$). An ordered particle with Pt (001) facets has an increased concentration of Pt atoms in the surface layer and is therefore energetically favored over a particle with Fe (001) facets. In contrast, simulations with the parameter h set to zero showed that in this case the occurrence of Fe or Pt (001) facets depends on the composition: For $h=0$, particles with an excess of Fe atoms then always exhibit Fe (001) facets, as this allows them to accommodate some of the excess Fe atoms in the surface layer without introducing disorder. For the same reason, particles with an excess of Pt atoms always possess Pt (001) facets for $h=0$.

As can already be seen in Fig. 6, a large fraction of excess atoms in particles with nonideal composition segregate on the particle surface. For particles with an excess of Fe atoms, Fe segregates preferentially on the Pt (001) facets, forming an ordered superstructure corresponding to the (100) and (010) facets [Figs. 6(a) and 6(b)]. Segregation of Pt in particles with an excess of Pt atoms [Figs. 6(d) and 6(e)] starts at the edges of the TO. Once the edges are occupied almost entirely by Pt atoms, segregation can also be observed on the (111) and (100) facets, the last showing an almost complete coverage with Pt for high Pt concentrations [Fig. 6(e)].

The energies for replacing an Fe atom by an excess Pt atom at various sites of an ordered particle are listed in Table IV. From this table, it is evident why excess Pt atoms first segregate on the edges of Pt rich particles: Replacing an Fe atom by a Pt atom at an edge site costs the least amount of energy. However, the tabulated energies cannot explain why Pt occupies only every second site on the (111) facets, while the (100) facets are almost completely covered with Pt. The reason for this is that Table IV only lists the energies for replacing an Fe atom that has a completely ordered surrounding. If the atom already has a Pt atom occupying a wrong lattice site in its neighborhood, the energy for replacing this atom increases for the case of the (111) facet to $10J_1-\frac{3}{2}h-6J_2=0.7485$ eV, while it decreases for the (100) facet to $8J_1-\frac{4}{3}h-6J_2=0.6278$ eV. Therefore, it becomes more favorable for Pt atoms to occupy (100) facets with increasing level of segregation.

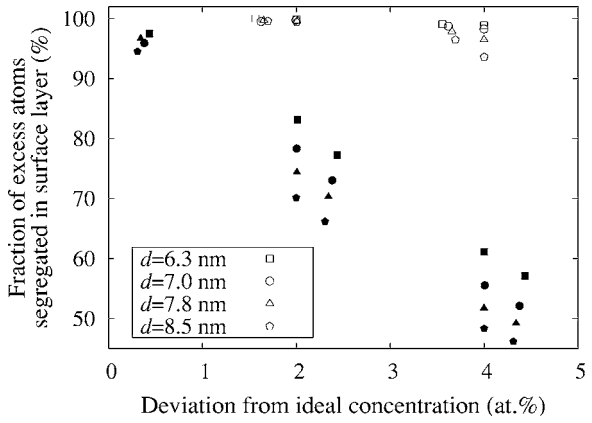

FIG. 7. Analysis of the surface segregation behavior. The fraction of excess atoms segregating on the surface is plotted over the deviation of the particle composition from the respective ideal composition. Open symbols: particles with excess Pt, solid symbols: particles with excess Fe.

The amount of surface segregation for both Fe and Pt atoms is analyzed quantitatively in Fig. 7, where the fraction of excess atoms segregated on the surface layer is plotted over the deviation of the overall particle composition from the composition of an ideally ordered regular TO. It is shown that virtually all excess Pt atoms are located at the surface, leaving the bulk of the particle at the ideal composition. The situation is different for particles enriched with Fe, where the surface can only accommodate a small number of excess Fe atoms. For larger deviations from the ideal composition, a considerable amount (up to approximately 50%) of excess Fe remains in the volume of the particles.

B. Influence of particle composition on the ordering behavior

In Fig. 8, the ordering behavior of 7 nm particles with Pt concentrations deviating from the ideal composition is depicted. For all other particle sizes, the composition dependence of ordering is qualitatively the same and is therefore not shown here.

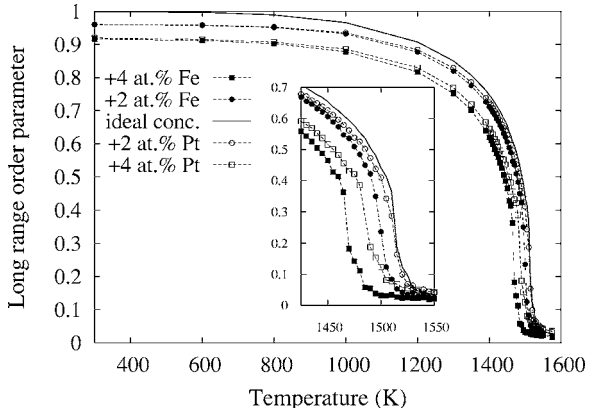

FIG. 8. Dependence of ordering on temperature for particles with different composition. The size of the particles is 7 nm. The inset shows a magnification of the region around the order-disorder transition.

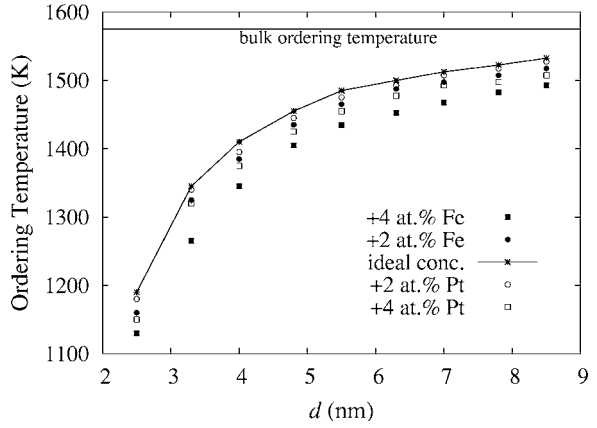

FIG. 9. Dependence of ordering temperature on particle size and composition.

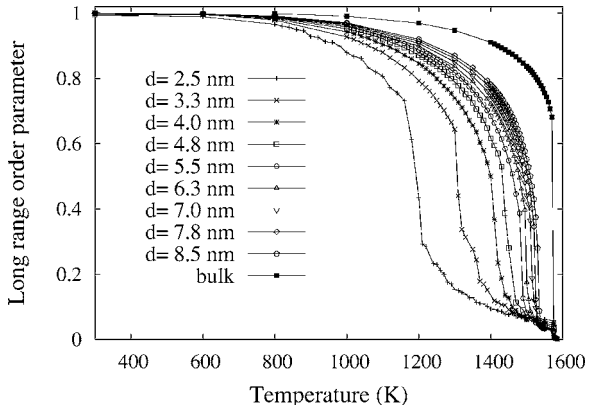

FIG. 10. Dependence of ordering on temperature for different sized particles. All particles possess the the respective ideal composition of an ordered regular TO. For comparison, the curve of the $Fe_{50}Pt_{50}$ bulk sample is also shown.

Excess atoms in ordered particles with non-ideal composition have to occupy sites of a wrong sublattice and therefore inevitably lead to disorder in the particle. In effect, particles with nonideal composition cannot attain a completely ordered structure at low temperatures, as can be seen in Fig. 8.

Also, Fig. 8 shows that the transition from the disordered to the ordered phase is shifted towards lower temperatures with increasing deviation from the ideal composition. For a quantitative comparison, the ordering temperatures of the particles have been determined and are shown in Fig. 9. Since the order-disorder transition in the particles is widened over a temperature interval, we define the ordering temperature as the temperature corresponding to the highest slope in the LRO over temperature plots.

From Fig. 9, it is apparent that the reduction of ordering temperature is more pronounced for particles enriched with Fe than for particles enriched with Pt. For example, the ordering temperature of the particle with an excess of Pt atoms of 2 at. % is only slightly decreased compared to the ordering temperature of the particle with ideal composition. In contrast, the particle with an excess of Fe atoms of 2 at. % shows a clear reduction of the ordering temperature of about 20 K.

The fact that particles with an excess of Fe atoms exhibit a stronger reduction of the ordering temperature than particles with an excess of Pt atoms can be explained by the different surface segregation behaviors of Fe and Pt. As was demonstrated in the last section, almost all excess Pt atoms segregate on the particle surface, while a considerable fraction of excess Fe remains in the volume of Fe rich particles. From the definition of the LRO parameter in Eqs. (6) and (7), it follows that the amount of disorder introduced by an excess atom itself is independent from whether it occupies a surface or a bulk site. However, an atom occupying a wrong lattice site favors the introduction of additional disorder in its surrounding. For example, the energy required to exchange two neighboring Fe and Pt atoms on a completely ordered lattice is $12J_1-24J_2$ (0.7812 eV with the current parameter set). If another atom occupying a wrong lattice site is in the nearest neighborhood of one of the two atoms and in the next nearest neighborhood of the other atom, this energy is reduced to $8J_1-20J_2$ (0.558 eV). As a consequence of its higher coordination, an excess Fe atom in the volume facilitates the exchange of a larger number of pairs than an excess Pt atom on the surface. It will therefore lead to a higher degree of disorder, which explains the larger reduction of the ordering temperature.

At low temperatures, the energy required to exchange a pair of atoms even in the neighborhood of an excess atom is large enough to efficiently suppress the exchange. Therefore, the ordering in the particles tends towards the maximum possible amount at the given composition and the residual disorder at low temperatures is independent from the type of the excess atoms, as can be seen in Fig. 8.

C. Influence of particle size on the ordering behavior

For investigating size effects on the ordering behavior, particles with varying size and respective ideal composition were compared. In Fig. 10, the dependence of long-range order on temperature for nanoparticles and a $Fe_{50}Pt_{50}$ bulk sample is depicted. Independent from size, all particles reach complete ordering at low temperatures. The order-disorder transition of the particles, however, is shifted towards lower temperatures with decreasing particle size as shown in Fig. 9. The ordering temperature of the largest particle (8.5 nm, 1530 K) is lowered by approximately 40 K compared to the bulk sample (1573 K). The ordering temperature of the smallest particle (2.5 nm, 1190 K) is lowered by approximately 380 K.

The decrease of the ordering temperature when going from the bulk to small particles is due to the presence of surface atoms. Their low coordination reduces their driving force for occupying ordered lattice sites and disorder is introduced more easily in the system. When proceeding to even smaller particles, the surface to volume ratio increases. Additionally, the mean coordination of the surface atoms is further reduced. Both effects explain the further decrease of ordering temperature with decreasing particle size.

The decrease of ordering temperature for nanometer sized particles in our model is comparatively small. Even for the

smallest particles considered (2.5 nm), the order-disorder transition occurs at a temperature as high as 1190 K. Typical annealing temperatures for inducing a transformation from the disordered to the $L1_0$ ordered phase in 6 nm FePt nanoparticles are 800 K.[21] Our simulations therefore give no evidence that the lack of ordering found in FePt nanoparticles even after thermal annealing originates in a decrease of the thermodynamical ordering temperature due to a high ratio of surface energy to volume free energy. However, it should be kept in mind that for particle sizes smaller than approximately 6 nm, twinning can occur, which is not described by our model.

D. Influence of the degree of surface segregation on the ordering behavior

As described in Sec. III B, the model parameter h has been fitted against an experimental value for Pt surface segregation in an $Fe_{20}Pt_{80}$ alloy. The uncertainty of this value (96 ± 4 at. %) in principle allows for a wide range of parameters h, spanning from $h=0$ (no driving force for surface segregation) to high values of h that would correspond to an almost complete coverage of the (111) surface of the $Fe_{20}Pt_{80}$ alloy with Pt. Also, depending on the preparation process, FePt particles can also be dispersed in a matrix or coated by organic ligands. These different chemical surroundings can significantly alter the surface segregation behavior, which can be reflected in our model by choosing different values for the parameter h. Preferential segregation of one element distorts the stacking sequence imposed by the $L1_0$ order on the surface and depletes the bulk of the particle of the segregating element. Therefore, a strong interplay between surface segregation and ordering can be expected and it is of interest to examine the influence of the parameter h on the order in the particles.

In the following, we investigate the influence of the parameter h on the ordering behavior by concentrating on FePt particles that have been synthesized by a wet chemical process as described in Ref. 1. The so-prepared particles are coated by organic ligands consisting of oleic acid molecules. In contrast to FePt particles prepared from the gas phase, no multiply twinned icosahedral shapes are observed in the wet chemically synthesized particles. Instead, the truncated octahedral shape is found for particles as small as 3 nm.[4] Therefore, fixing the particle shape to a regular TO does not restrict the applicability of our model to particles larger than a certain critical size.

If one assumes that the oleic acid molecules bind more strongly to the Fe than to the Pt atoms by partial oxidization, a reversal of the surface segregation behavior towards a preferential segregation of Fe atoms can be expected. For our model, this implies a positive sign of the parameter h. Also, by replacing oleic acid with other molecules, the degree of Fe surface segregation should in principle be tunable.

For a particle with a diameter of 4 nm (2406 atoms) and corresponding ideal composition (50.71 at. % Fe), we controlled the degree of Fe surface segregation by varying the parameter h between 0 and 2.4 eV (see Fig. 11). For $h \leqslant 0.3$ eV, the driving force for ordering overcomes the tendency for surface segregation and the concentration of Fe in the surface corresponds to the concentration imposed by a complete $L1_0$ ordering of the particle. With increasing h, the content of Fe in the surface layer is raised. For $h \geqslant 2.1$ eV, the tendency for surface segregation has become so large that the entire surface of the particle is covered with Fe atoms. For each value of h, the degree of order in the particle has been analyzed by counting the fraction of atoms whose nearest neighbor sites are occupied according to the $L1_0$ structure.[22] The results are shown in Fig. 11. Starting with an almost completely ordered particle for low values of h, the amount of $L1_0$ ordering decreases with increasing surface segregation of Fe. In the limiting case of a completely Fe terminated particle surface, only 9% of the atoms can order in the $L1_0$ structure.

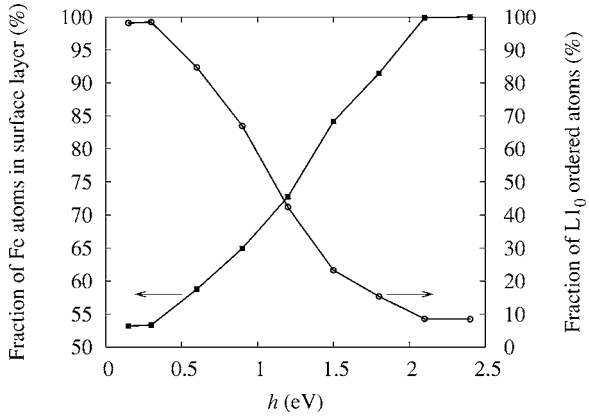

FIG. 11. Dependence of the degree of surface segregation and $L1_0$ ordering on the parameter h for a 4 nm particle with ideal composition ($T=300$ K).

Out of the 2406 atoms of the 4 nm particle, 752 atoms occupy surface sites. If all the surface sites are occupied by Fe atoms, the composition of the remaining particle bulk is shifted towards approximately 72 at. % Pt. This leads to a suppression of $L1_0$ ordering in the particle, as the bulk composition lies outside the stability region of the $L1_0$ phase. Instead, a simultaneous evolution of $L1_2$ ordered domains can be expected. This is confirmed by analyzing the structure of completely Fe terminated particles in more detail, as is shown in Fig. 12. In the left column of Fig. 12, cross sections of different sized completely Fe terminated particles are presented. Beneath the surface Fe layer, all particles exhibit a layer almost completely occupied by Pt atoms. In the remaining bulk of the particles, $L1_0$ and $L1_2$ ordered areas can easily be identified, as it is indicated by the light and dark gray patches in the right column of Fig. 12. The bulk of the smallest particle presented (3.3 nm) is completely $L1_2$ ordered. Here, the shift of the bulk composition is most important. In the 4 nm particle, the main fraction of bulk atoms are still $L1_2$ ordered. However, small $L1_0$ ordered domains evolve in the center and at the (100) surfaces of the particle. With further increasing particle size, an $L1_0$ ordered domain spans over the whole particle in [001] direction and grows at the expense of the $L1_2$ ordered areas. In the largest particle displayed (6.3 nm), the bulk is almost completely $L1_0$ ordered and no $L1_2$ domains can be identified.

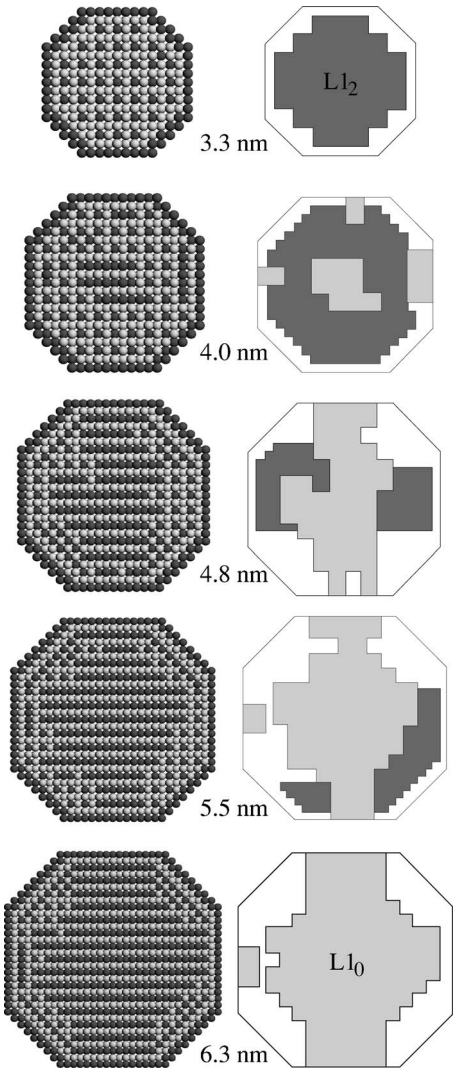

FIG. 12. Left column: Cross sections of completely Fe terminated particles with overall composition close to stoichiometry (T =300 K, h=2.4 eV). Right column: Dark gray patches indicate $L1_2$ ordered domains, light gray patches indicate $L1_0$ ordered domains.

The amount of $L1_0$ ordering of particles with complete Fe surface segregation is analyzed quantitatively in Fig. 13. As was already observed in Fig. 12, the surface segregation suppresses the $L1_0$ ordering completely in particles with diameter $d \leqslant 3.3$ nm. In contrast, in the largest particle analyzed (7.0 nm), 40% of the atoms are found to be $L1_0$ ordered. The value of 40% ordering in the 7 nm particle seems to be rather small when compared to the large $L1_0$ ordered domain visible even in the 6.3 nm particle of Fig. 12. However, in the quantitative analysis, only those atoms are counted as ordered that have a completely ordered nearest neighborhood. This excludes all atoms at the boundaries of a domain and explains the apparent discrepancy.

The reduction of $L1_0$ ordering by surface segregation is largely due to the shift of the bulk composition. Therefore, an increase of the overall concentration of the segregating element can restore the stoichiometric composition in the bulk and can thus promote the ordering in the particles. The effect of increasing the Fe content of completely Fe terminated 4 nm particles on the degree of $L1_0$ ordering is shown in Fig. 14. As expected, the amount of ordering increases with increasing Fe concentration. The fraction of the particle that is $L1_0$ ordered reaches its maximum of approximately 44% at a composition of 62 at. % Fe. This value is conserved up to a composition of 65 at. % Fe. For higher concentrations of Fe, the order is again reduced.

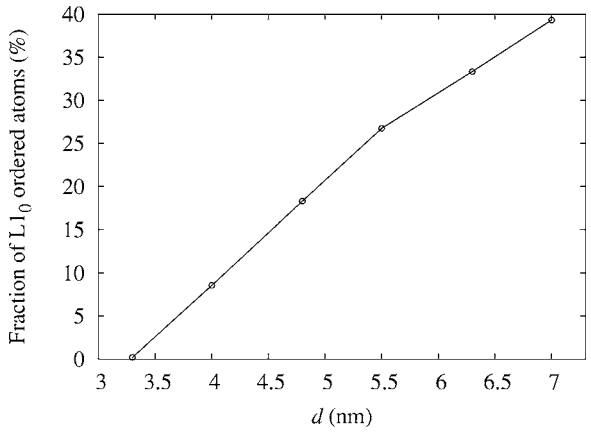

FIG. 13. Dependence of $L1_0$ ordering on particle size in completely Fe terminated particles with overall composition close to stoichiometry.

In order to restore the stoichiometric composition of FePt in the bulk of a completely Fe terminated 4 nm particle, an overall concentration of approximately 65 at. % Fe is needed. Therefore, instead of the observed plateau, the degree of order should be expected to have a distinct maximum at 65 at. % Fe. The presence of the plateau can be explained by examining the cross sections of the particles at the limits of the plateau, as shown in the insets of Fig. 13. At 62 at. % Fe, the particle consists of an outer Fe shell, followed by a complete Pt shell. The remaining bulk of the particle is a single $L1_0$ ordered domain. For increasing the order with further addition of Fe atoms, the Fe layers of the ordered domain would have to break through the surrounding Pt shell. At 65 at. % Fe, this breaking through is observed only at the (111) facets of the particle. At the (100) facets perpen-

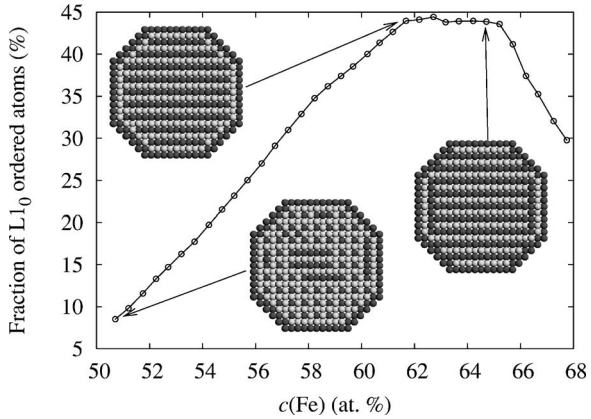

FIG. 14. Dependence of $L1_0$ ordering on composition in completely Fe terminated particles with a diameter of 4 nm. The insets show cross sections of particles at distinct compositions.

dicular to the ordered direction, Fe is incorporated into the third layer and an antiphase boundary is developed. The disorder introduced by the antiphase boundary keeps the overall order in the particle at a constant level when increasing the Fe content from 62–65 at. %.

The simulations with varying h show a strong dependence of the maximum degree of order attainable in a particle and the tendency of one element to segregate on the surface. For stoichiometric particles smaller than approximately 4 nm, complete segregation of one element suppresses the formation of $L1_0$ order entirely. By increasing the concentration of the segregating element and thus restoring the stoichiometric composition in the bulk, the order in the particles can be enhanced.

V. CONCLUSION

We investigated thermodynamic properties of nanometer sized FePt particles by Monte Carlo simulations. In particular, the influence of particle size, particle composition and surface segregation on the ordering behavior has been analyzed. The Monte Carlo simulations employ a an Ising-type Hamiltonian on a rigid lattice with NN and NNN pair energies for describing the atom-atom interaction. The parameters of the model have been determined by fitting against the FePt bulk phase diagram and experimental data on Pt surface segregation.

The key findings of these simulations can be summarized as follows.

(1) The simulations give no evidence for a considerable reduction of the thermodynamic ordering temperature of free particles with decreasing particle size. They therefore suggest that the lack of chemical ordering found in FePt particles under a certain critical size cannot be attributed to a reduction of the ordering temperature by the high ratio of surface energy to volume free energy.

(2) The reduction of ordering temperature with increasing deviation from the stoichiometric composition has been found to be more pronounced for Fe-rich particles than for Pt-rich particles. This observation can be explained by the strong surface segregation tendency of excess Pt atoms, while a large amount of excess Fe atoms was found to remain in the volume of the particles.

(3) A strong dependency of ordering on the degree of surface segregation has been demonstrated. If complete surface segregation of one element is assumed, we observe increasing disorder with decreasing particles size and the formation of $L1_2$ domains. Ordering in the particles can be restored, however, by increasing the concentration of the segregating element. The observed dependence of internal ordering on surface energetics can therefore provide another possible explanation for the reduction of ordering with particle size for supported and matrix embedded particles, as observed, e.g., by Hono *et al.*[5]

ACKNOWLEDGMENTS

We acknowledge generous grants for computing time by the Center for Scientific Computing at the Johann Wolfgang Goethe-University, Frankfurt, Germany. We are thankful to Dipl.-Ing. Jens Ellrich, TU Darmstadt, and Dr. B. Rellinghaus, IFW Dresden, for fruitful discussions. Financial support by the German foreign exchange service (DAAD) through a bilateral travel program is gratefully acknowledged.

*Electronic address: mueller@mm.tu-darmstadt.de

[1] S. Sun, C. B. Murray, D. Weller, L. Folks, and A. Moser, Science **287**, 1989 (2000).
[2] B. Bian, D. E. Laughlin, K. Sato, and Y. Hirotsu, J. Appl. Phys. **87**, 6962 (2000).
[3] S. Stappert, B. Rellinghaus, M. Acet, and E. F. Wassermann, J. Cryst. Growth **252**, 440 (2003).
[4] B. Stahl, J. Ellich, R. Theissman, M. Ghafari, S. Bhattacharya, H. Hahn, N. S. Gajbhiye, D. Kramer, R. N. Viswanath, J. Weissmüller, and H. Gleiter, Phys. Rev. B **67**, 014422 (2003).
[5] Y. K. Takahashi, T. Koyama, M. Ohnuma, T. Ohkubo, and K. Hono, J. Appl. Phys. **95**, 2690 (2004).
[6] K. Binder, J. L. Lebowitz, M. K. Phani, and M. H. Kalos, Acta Metall. **29**, 1655 (1981).
[7] Since the equilibrium structures at two successive temperatures only differ slightly in general, this procedure reduces the number of MC steps needed to initially equilibrate the system at each temperature.
[8] K. Binder, Phys. Rev. Lett. **45**, 811 (1980).
[9] D. F. Styer, M. K. Phani, and J. L. Lebowitz, Phys. Rev. B **34**, 3361 (1986).
[10] *Landolt-Börnstein: Numerical Data and Functional Relationships in Science and Technology*, edited by H. Ullmaier (Springer-Verlag, Heidelberg, 1991), No. 5.
[11] P. Beccat, Y. Gauthier, R. Baudoing-Savois, and J. C. Bertolini, Surf. Sci. **238**, 105 (1990).
[12] C. Creemers and P. Deurinck, Surf. Interface Anal. **25**, 177 (1997).
[13] L. D. Marks, Rep. Prog. Phys. **57**, 603 (1994).
[14] F. Baletto and R. Ferrando, Rev. Mod. Phys. **77**, 371 (2005).
[15] C. L. Cleveland and U. Landman, J. Chem. Phys. **94**, 7376 (1991).
[16] J. Uppenbrink and D. J. Wales, J. Chem. Phys. **96**, 8520 (1992).
[17] D. Reinhard, B. D. Hall, P. Berthoud, S. Valkealahti, and R. Monot, Phys. Rev. B **58**, 4917 (1998).
[18] K. Koga, T. Ikeshoji, and K. I. Sugawara, Phys. Rev. Lett. **92**, 115507 (2004).
[19] Z. R. Dai, S. Sun, and Z. L. Wang, Surf. Sci. **505**, 325 (2002).
[20] B. Rellinghaus, S. Stappert, M. Acet, and E. F. Wassermann, J. Magn. Magn. Mater. **266**, 142 (2003).
[21] Z. R. Dai, S. Sun, and Z. L. Wang, Nano Lett. **1**, 443 (2001).
[22] The LRO parameter introduced in Sec. II is not appropriate for describing the degree of $L1_0$ of order in particles with a high tendency for surface segregation. The shift of the bulk composition leads to a partial $L1_2$ ordering (see Fig. 12), which also has a nonzero contribution to the LRO parameter.